

## The laser calibration system of the HARP TOF

A. Andreoni<sup>a</sup>, M. Bondani<sup>a</sup>, M. Bonesini<sup>b</sup>, F. Ferri<sup>b</sup>, D. Gibin<sup>c</sup>, P. Govoni<sup>b</sup>, A. Guglielmi<sup>c</sup>,  
A. Menegolli<sup>c</sup>, M. Paganoni<sup>b</sup>, F. Palestini<sup>b</sup>, A. Parravicini<sup>b</sup>, A. Sottocornola-Spinelli<sup>a</sup>, A. Tonazzo<sup>b</sup> \*

<sup>a</sup>Dip. di Scienze Chimiche e Fisiche, Università dell' Insubria, via Valleggio 11, Como, Italy

<sup>b</sup>INFN – Sezione di Milano, Dip. di Fisica “G. Occhialini”, Pza. Scienza 3, Milano, Italy

<sup>c</sup>INFN – Sezione di Padova, Dip. di Fisica “G. Galilei”, via Marzolo 8, Padova, Italy

The calibration and monitoring system constructed for the HARP experiment scintillator-based time of flight system is described. It is based on a Nd-Yag laser with passive Q-switch and active/passive mode-locking, with a custom made laser light injection system based on a bundle of IR monomode optical fibers. A novel ultrafast InGaAs MSM photodiode, with 30 ps risetime, has been used for the laser pulse timing. The first results from the 2001-2002 data taking are presented, showing that drifts in timing down to about 70 ps can be traced.

### 1. Introduction

The HARP experiment [1], shown schematically in figure 1, is devoted to the study of hadroproduction on nuclear targets for incident beam momenta between 2 and 15 GeV/c, the energy range of interest for atmospheric neutrinos and the neutrino factory design. It has been taking data at CERN, on the PS T9 beamline, in 2001 and 2002, and has now completed its programme. The HARP spectrometer provides track reconstruction and particle identification over the full solid angle. In the forward direction, particle identification is performed at low momenta ( $p \leq 3.5$  GeV/c) by a scintillator based TOF Wall and at high momenta by a threshold Cerenkov counter.

The requirements for the forward TOF Wall include excellent timing resolution, for particle identification, and good transverse segmentation to avoid particle pile-up on single counters. The system specifications called for a time resolution of  $\sigma \simeq 250$  ps to separate at  $4\sigma$  pions from protons up to 3.5 GeV/c, on the basis of a 10 m flight path. Particle identification is achieved combining leading-edge time measurements (from TDC)

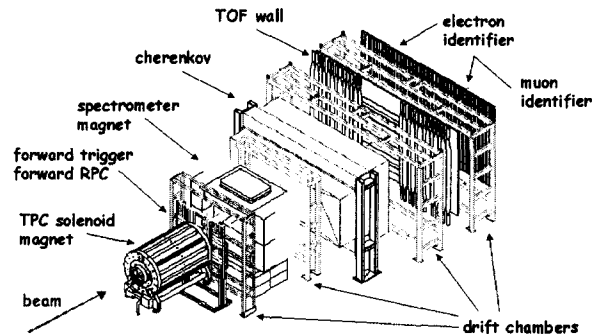


Figure 1. Layout of the HARP experiment at the CERN PS. The different sub-detectors are shown. The target is inserted inside the TPC. The TOF Wall is located about 10 m downstream of the target station.

with pulse-height information for time-walk corrections (from ADC).

The HARP TOF Wall covers a total area of about  $7.4 \times 2.5$  m<sup>2</sup>. The size of the individual scintillator (BC408 from Bicron) bars are  $2.5 \times 21 \times 180$  (250) cm<sup>3</sup> in the central (left/right) palizades, where they are laid horizontally (vertically).

\*Corresponding author. e-mail: Alessandra.Tonazzo@cern.ch. Now at Università di Roma Tre, Dip. di Fisica “E. Amaldi”, via della Vasca Navale 84, Rome, Italy

Each counter is read by two photomultipliers (Philips XP2020) at the two ends.

The analog signal is fed, after a 40 m long RG-213 cable, to an active splitter chain in the counting room, that divides the signal 25% to the ADC line<sup>2</sup> and 100% to the TDC line<sup>3</sup>, after a leading edge discriminator<sup>4</sup>.

For a particle crossing at a time  $t_0$  a scintillator bar (equipped with two photomultipliers (PMT)  $i$  at the edges) at a distance  $x$  from its center, the time difference  $\Delta t_i$  between the STOP from the PMT  $i$  and the START from a reference counter  $t_s$  is given by:

$$\Delta t_i = t_0 + \frac{L/2 \pm x}{v_{eff}} - t_s + \delta_i \quad i = 1, 2$$

where  $L$  is the scintillator length,  $v_{eff}$  the effective light velocity in the scintillator bar ( $v_{eff}^{-1} \approx 5.9$  ns/m) and  $\delta_i$  includes all delays (cables, PMT transit time, ...). The quantity  $\Delta t_+ = \frac{\Delta t_1 + \Delta t_2}{2} = t_0 + \frac{L}{2 \cdot v_{eff}} - t_s$  is independent of the impact point  $x$  along the counter and allows to measure the time of flight, while the impact position  $x$  can be deduced from  $\Delta t_- = \frac{\Delta t_1 - \Delta t_2}{2} = \frac{x}{v_{eff}}$ .

The resolution of PMT  $i$  is given by  $\sigma_i^2 = \sigma_{\Delta t_i}^2 - \sigma_{t_s}^2$ , while the crossing time ( $t_0$ ) resolution is given by  $\sigma_0 = \frac{1}{2} \sqrt{\sigma_1^2 + \sigma_2^2}$  and is expected to be equivalent to the one calculated directly from the distribution of  $\Delta t_-$ .

Drifts in delays are to be included in the calibration constants  $\delta_i$ , that must be equalized at the beginning of the data taking period.

The intrinsic resolution of the scintillator counters of the TOF Wall has been preliminary evaluated to be around 160 ps. This puts severe constraints on the calibration system, especially on the laser monitoring system: timing drifts have to be traced down at better than 100 ps.

Accurate equalization of the time response of the different counters is achieved with two methods: cosmic calibrations [3], which are repeated every 2-3 months and provide average values of the calibration constants, and a laser system, which allows for continuous monitoring of the

evolution of the equalization constants, on a daily basis.

## 2. Hardware structure of the laser calibration system

A layout of the laser calibration system constructed for the HARP TOF Wall is shown in figure 2. Given the requirement to spot out time drifts of the TOF system at the level of 1-2 TDC counts, i.e. down to 70 ps, all the elements of the system (laser source, optoelectronic fiber system, fast photodiode for TDC start, injection system into the single scintillator bars) had to be carefully chosen.

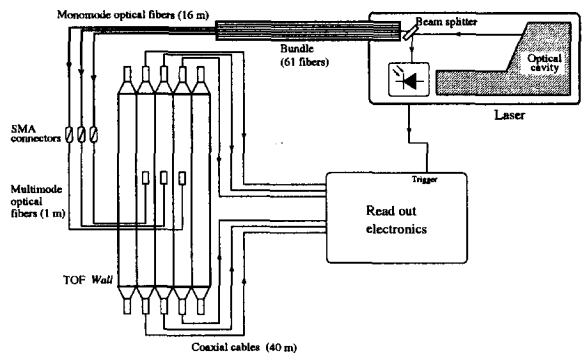


Figure 2. Layout of the laser calibration system for the HARP TOF Wall.

For the light source of the monitoring system we used a custom made Nd-Yag laser<sup>5</sup> with passive Q-switch, active/passive mode locking and 10 Hz repetition rate. The infrared (IR) emission (at  $\lambda = 1064$  nm) is converted into a second harmonic at 532 nm by a KD\*P SHG crystal. The Q-switch, to obtain short and powerful laser pulses, is obtained via a dye (Exciton Q-switch I from Kodak, diluted in dicloro-ethane). According to the manufacturer's specifications, the laser had an output pulse width in the IR of  $\sim 60$  ps

<sup>2</sup>based on CAEN V792, 12 bit, 32 channel modules

<sup>3</sup>based on CAEN V775, 12 bit, 32 channel modules

<sup>4</sup>model Lecroy 4413, 16 channels

<sup>5</sup>modified SYLP0 from Quanta Systems srl, Via Venezia Giulia 28, Milano, Italy

(FWHM) and an average energy per pulse of  $\sim 6$  mJ, with an energy stability of  $\pm 5\%$  for 95% of the shots. The laser pulse average energy has been checked with a pyroelectric device<sup>6</sup>, confirming the manufacturer's specifications.

The pulse width (and as a consequence the sharpness of the leading edge) is an essential point for our system, and the manufacturer's specifications were verified for various concentrations of the dye solution. The IR laser pulse width, before KD\*P second harmonic generation, was directly measured with an optical technique based on autocorrelation [4]. The results of the measurements were in good agreement with the manufacturer's specification.

In the calibration system, the laser light is beam splitted to a fast photodiode, providing the start for the TDC system, and to a bundle of fibers that transmit the pulse to the different scintillator channels.

In order to take full advantage of the high-speed nature of our laser source, the device for timing the light pulse (and so giving the TDC start) must also be very fast. For this purpose we used a novel design InGaAs Metal-Semiconductor-Metal (MSM) photodetector<sup>7</sup> with 30 ps rise and fall time, a low dark current of  $\sim 100$  pA,  $0.2 \times 0.2$  mm<sup>2</sup> sensitive area and a good radiant sensitivity between 450 and 850 nm.

Due to the wide area covered by the TOF Wall and the requirement to have the laser source out of the experimental area for easy handling during beam data taking periods, relatively long fibers ( $\sim 15$  m) had to be used to inject the laser light into the single scintillator counters of the TOF Wall.

The choice of the type of optical fiber in the bundle was a critical issue. Precise timing requires a minimum modification to the time characteristics of the fast injected laser pulse or more precisely that the leading edge of the pulse (on which discrimination is done) has a minimum jitter, therefore monomode fibers would be the optimal choice; however, light injection into the nar-

row core of such fibers is a quite delicate task. To reduce injection problems, we used larger core diameter IR monomode fibers, that for green light behave as a "limited number of modes" fiber. The choice of the fiber type was based on the measurement of the additional spread introduced on the shape of a laser pulse. Corning SMF-28 fibers (see table 1 for details) were chosen for the fibre bundle.

|  |  |
|--|--|
| core diameter                              | 8.2 $\mu\text{m}$  |
| numerical aperture                         | 0.14   |
| zero dispersion wavelength ( $\lambda_0$ ) | 1312 nm  |
| zero dispersion slope                      | 0.090 ps/(nm $\times$ km)  |
| dispersion $D(\lambda)$                    | $\frac{S_0}{4} [\lambda - \frac{\lambda_0^4}{\lambda^3}]$ ps/(nm $\cdot$ km)<br>(1200 $\leq \lambda \leq$ 1600 nm) |
| refr. index difference                     | 0.36%  |

Table 1  
Characteristics of the IR monomode Corning SMF-28 fibers.

The bundle consisted of 61 fibers (15 m long) cut at one edge, peeled and encapsulated in an optical cement matrix and then polished at the free surface. The other end, after about 1 m, is completely free and has individual optical SMA connectors. Before the injection in the fiber bundle, the laser light is attenuated by a system of optical neutral filters<sup>8</sup> (OD  $\sim 4.5$ ) to make the scintillator signal from laser light similar to the one from a minimum ionizing particle (MIP), and the laser beam spot is enlarged (to about 5 mm diameter) by a system of lenses to reduce intensity disuniformities.

At the free end of each fiber the laser signal is injected into a short (1m long) multimode fiber<sup>9</sup> that ends in a small prism glued at the center of each scintillator bar. The use of a multimode fiber (with a bigger numerical aperture: 0.22) allows for the injection of the laser light into the scintillator bar at a direction closer to the PMT

<sup>6</sup>model Gentec ED-200

<sup>7</sup>Hamamatsu G4176

<sup>8</sup>Solid Glass ND filters, from Ealing Electro-optics

<sup>9</sup>CERAM OPTEC UV 100/125

axis (after first light reflection), giving a calibration signal which is faster and more similar to the one from cosmic rays muons.

### 3. Measurement of single counter timing resolution

The time resolution of the TOF Wall counters has been measured both with dedicated cosmic rays runs during construction [2], and with the laser system in situ. The laser light is injected into the center of each scintillator slab and the time recorded in both PMT. Time walk corrections are applied to reduce the dependence of the timing response on the signal amplitude, and ADC signals with averages compatible with a MIP are selected. However, some care has to be taken in the comparisons, due to the different mechanisms involved in the light generation. The time resolution can be evaluated plotting the quantity  $\Delta t_-$  for each slab, with dedicated laser runs. The obtained average intrinsic resolutions, as determined with the laser system, for all the TOF Wall counters are:

$$\sigma_L(L = 250 \text{ cm}) = 143 \pm 31 \text{ ps}$$

$$\sigma_L(L = 180 \text{ cm}) = 126 \pm 26 \text{ ps}$$

consistent with the values from cosmic ray runs.

The method used with the laser eliminates all contributions to timing resolution, which are common to both PMT's, including any jitter in the photodiode reference time.

### 4. Comparison with the cosmic rays calibration

The TOF Wall was calibrated at regular intervals, about every month or two during PS MD periods, with cosmic rays muons. The calibration procedure is quite lengthy (about 3 days of data taking) and cannot be performed more frequently. These calibrations are used to determine the initial values of the equalization constants  $\delta_i$  at time  $T_0$  and to make periodic recalibrations.

The reliability of the time monitoring performed with the laser system was checked by comparing the variation of the time equalization

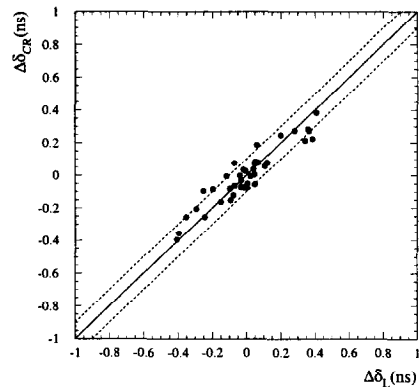


Figure 3.  $\Delta\delta_{CR}$  are the drifts in the delay constants of each channel as measured with incoming cosmic ray muons between May 2002 and November 2001.  $\Delta\delta_L$  are the same drifts as measured with the laser system. The rms of the difference of  $\Delta\delta_{CR}$  and  $\Delta\delta_L$  is less than  $\pm 70$  ps.

constants  $\delta_i$  obtained with cosmic rays calibration runs and laser calibration runs ( $\Delta\delta_{CR}$  vs  $\Delta\delta_{Laser}$ ).

Results from this comparison are shown in Figure 3, where the differences between the 2002 data taking startup (May 2002) and the end of the 2001 data taking period (November 2001) are plotted. Major interventions on the TOF Wall system took place in May 2002, resulting in changes of the time calibration constants  $\delta_i$  up to  $\pm 0.5$  ns, as measured with cosmic rays. These changes were well followed by the laser system, and the differences between the two systems are well within a  $\pm 100$  ps band.

### 5. TOF Wall time stability

The laser system is essential to monitor the TOF Wall stability daily over all the data taking period. The TDC time differences  $\Delta t_i(T)$ , measured at time T of the data taking period and corrected for time walk, have been studied for all PMT channels. There has been no evidence for time drift in excess of  $\sim 100$  ps over the full 2001

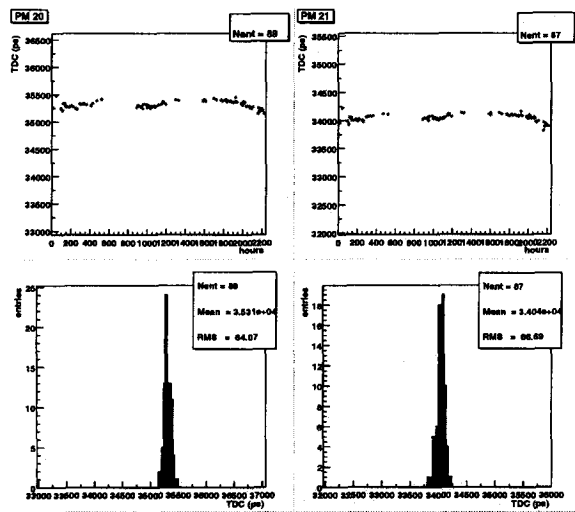


Figure 4. Variation of  $\Delta t$  vs running time  $T$  (2001 data taking: 3 months) for two typical PMT channels.

data taking period (3 months).

Figure 4 shows the behaviour for two typical channels, as a function of the running time  $T$ . The distribution of the rms  $\sigma_{\Delta t}$  for the individual channels of the TOF Wall, monitored after the full 2001 data taking period, is shown in figure 5. Possible drifts in the calibration constants  $\delta_i$  of the TOF Wall system due to temperature effects on a night-day timescale have been studied. No clear effects are seen, showing that the TOF Wall system is stable within the limits quoted above.

## 6. TOF Wall performance for particle identification

Particle identification in the HARP TOF Wall relies on the combination of particle momenta, as measured by the forward drift chambers, and the time of flight between a start signal ( $t_s$ ) from a reference counter before the target (TOFB) and a stop signal from the TOF Wall itself. The calibration issues discussed above are essential for the quality of the extracted TOF PID and thus the determination of particle masses. After the calibration procedure,  $\pi$  and  $p$  are separated at

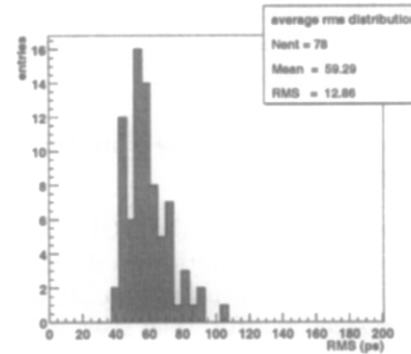


Figure 5. Histogram of the rms  $\sigma_{\Delta t}$  for all the TOF Wall PMT channels, monitored over the full 2001 data taking period.

better than  $5\sigma$  at 3 GeV/c incident momentum.

## 7. Conclusions

A fast-laser based calibration system has been developed for the time calibration and monitoring of a large TOF counters wall for the HARP experiment. The intrinsic TOF Wall resolution of  $\sim 160$  ps has put severe requirements on the calibration system. Time drifts down to about 70 ps can be monitored on a day by day timescale.

## REFERENCES

1. M.G. Catanesi et al., "Proposal to study hadron production for the neutrino factory and for the atmospheric neutrino flux", CERN-SPSC/99-35, SPSC/P315, 15 November 1999;  
M.G. Catanesi et al., "Status report of the HARP experiment", CERN-SPSC/2001-031, SPSC/M672, 29 October 2001.
2. G. Barichello et al., INFN/AE-02/01, 28 June 2002.
3. F. Bobisut et al., INFN/BE-02/03, 21 October 2002.
4. F. Zernike, J. Midwinter Applied Nonlinear Optics, J. Wiley, 1973